J Pharmacol Sci **108**, 505 – 516 (2008)

Journal of Pharmacological Sciences

Full Paper

Establishment and Characterization of Mammalian Cell Lines Stably Expressing Human L-Type Amino Acid Transporters

Emiko Morimoto[1], Yoshikatsu Kanai[1,2], Do Kyung Kim[1,3], Arthit Chairoungdua[1], Hye Won Choi[1], Michael F. Wempe[4], Naohiko Anzai[1], and Hitoshi Endou[1,5,*]

[1]*Department of Pharmacology and Toxicology, Kyorin University School of Medicine, Tokyo 181-8611, Japan*
[2]*Department of Pharmacology, Osaka University Graduate School of Medicine, Osaka 565-0871, Japan*
[3]*Department of Oral Physiology, Chosun University College of Dentistry, Gwangju, Korea*
[4]*Department of Pharmacology, James H. Quillen College of Medicine, East Tennessee State University, Johnson City, TN 37614-1708, USA*
[5]*J-Pharma Co., Ltd., Tokyo 160-0022, Japan*

Received September 1, 2008; Accepted October 27, 2008

Abstract. System L (SL), a basolateral amino acid transporter, transports large neutral amino acids (LNAAs) in a Na^+-independent manner. Previously, we identified two isoforms of transporters: L-type amino acid transporter 1 (LAT1) and 2 (LAT2) and revealed their distinct substrate selectivity and transport properties. In this study, to establish more stable human LAT1 (hLAT1) and LAT2 (hLAT2) in vitro assay systems, we established mouse cell lines stably expressing hLAT1 (S2-LAT1) and hLAT2 (S2-LAT2). Real-time quantitative RT-PCR analysis revealed that S2-LAT1 and S2-LAT2 cells express hLAT1 and hLAT2 mRNAs at 20 – 1000-fold higher levels than those of endogenous mouse Lat1 and Lat2. S2-LAT1 and S2-LAT2 mediated [^{14}C]L-leucine transport properties were measured and corresponded to results observed via *Xenopus* oocytes. Using these cells, the data demonstrate that hLAT1 and hLAT2 exhibit different characters in the acceptance of α-methyl amino acids and amino acid–related compounds with bulky side chains such as thyroid hormones and melphalan. S2-LAT1 and S2-LAT2 cells are expected to facilitate hLAT1 and hLAT2 substrate recognition research and contribute to drug development by providing an efficient assay system to screen for chemical compounds that interact with hLAT1 and hLAT2.

Keywords: amino acid transporter, system L (SL), SLC7, L-type amino acid transporter (LAT) 1, LAT2

Introduction

System L (SL), a basolateral amino acid transporter, transports large neutral amino acids (LNAAs) in a Na^+-independent manner (1, 2). SL plays a pivotal role in amino acid (AA) absorption via the small intestine and renal proximal epithelial cells (1). SL has been shown to support cell growth and proliferation in both normal and tumor cells (1, 3, 4). Furthermore, AA penetration through the blood-brain barrier (BBB) and placenta barrier (PB) utilize SL transporters (1). SL accepts many substrates including naturally occurring AA and AA-related compounds such as L-dopa, a therapeutic drug for Parkinsonism; melphalan, an anti-cancer phenylalanine mustard; thyroid hormones, triiodothyronine (T3) and thyroxine (T4); gabapentin, an anti-convulsant drug; and *S*-(1,2-dichlorovinyl)-L-cysteine, a neurotoxic cysteine conjugate (1, 5 – 10). Due to the various levels of endogenous SL activity present in cultured cells and tissue preparations, methodical compound SL interactions have thus far been limited. Therefore, in vitro models expressing specific SL transporters are required.

Using cDNA cloning, four SL transporter isoforms designated as L-type AA transporter 1 (LAT1), 2 (LAT2), 3 (LAT3), and 4 (LAT4) have been identified (11 – 14). Among these isoforms, LAT1 and LAT2 are

*Corresponding author (affiliation #1). endouh@kyorin-u.ac.jp
Published online in J-STAGE on December 10, 2008 (in advance)
doi: 10.1254/jphs.08232FP

predicted as 12-transmembrane proteins belonging to the hetero-dimeric AA transporter SLC7 family (3, 11, 12, 15 – 20). Required for functional expression in the plasma membrane, LAT1 and LAT2 require an additional single membrane spanning protein known as the 4F2 cell surface antigen heavy chain (4F2hc) (11, 12). LAT1 mediates Na^+-independent AA exchange and prefers LNAA substrates with bulky or branched side chains (11). Highly expressed in tumor cells, LAT1 supports growth by transporting AA (4, 21, 22). Present at the BBB and the PB, LAT1 likely contributes to the permeation of AAs and AA-related drugs through blood-tissue barriers (23 – 26). In contrast, LAT2 not only transports LNAA but also transports small neutral AAs. LAT2 is expressed more ubiquitously than LAT1 (12, 27, 28); LAT2 is highly expressed in the basolateral membrane of the small intestine and kidney epithelial cells (28).

LAT1 and LAT2 functional properties have been examined using the expressed *Xenopus laevis* oocyte model. However, a more ideal in vitro model to screen function and regulation requires mammalian cell sytems; establishing mammalian culture models may afford a more robust in vitro model (i.e., high through-put screening tools) over the oocyte model. Therefore, the present study describes our efforts to establish and characterize mouse cell lines stably expressing human LAT1 (hLAT1) and human LAT2 (hLAT2). We illustrate the following in this study: 1) that exogenously introduced hLAT1 and hLAT2 become expressed at fairly high levels and dominate over endogenous mouse LAT1 and LAT2, and 2) that the transport function of these stably transfected mammalian cell lines reflect the properties of exogenously introduced hLAT1 and hLAT2.

Materials and Methods

Materials

[^{14}C]L-Leucine was purchased from Du Pont NEN. Gabapentin and droxidopa were provided by Parke-Davis Pharmaceutical Research (Ann Arbor, MI) and Sumitomo Pharmaceutical Co., Ltd. (Osaka), respectively. Unless specifically indicated, the remaining compounds and reagents were purchased from Sigma-Aldrich Chemical Company (St. Louis, MO, USA). The chemical structures of AA-related drugs used in the present investigation are presented in Fig. 1.

Establishment of S2-LAT1 and S2-LAT2 cell lines

S2 cells were derived from transgenic mice harboring the temperature-sensitive simian virus 40 large T-antigen gene and cultured in RITC 80-7 medium (IWAKI, Tokyo) containing 5% FBS, 10 μg/ml transferrin, 0.08 U/ml insulin, and 10 ng/ml recombinant EGF (29). Cells were subcultured in a medium

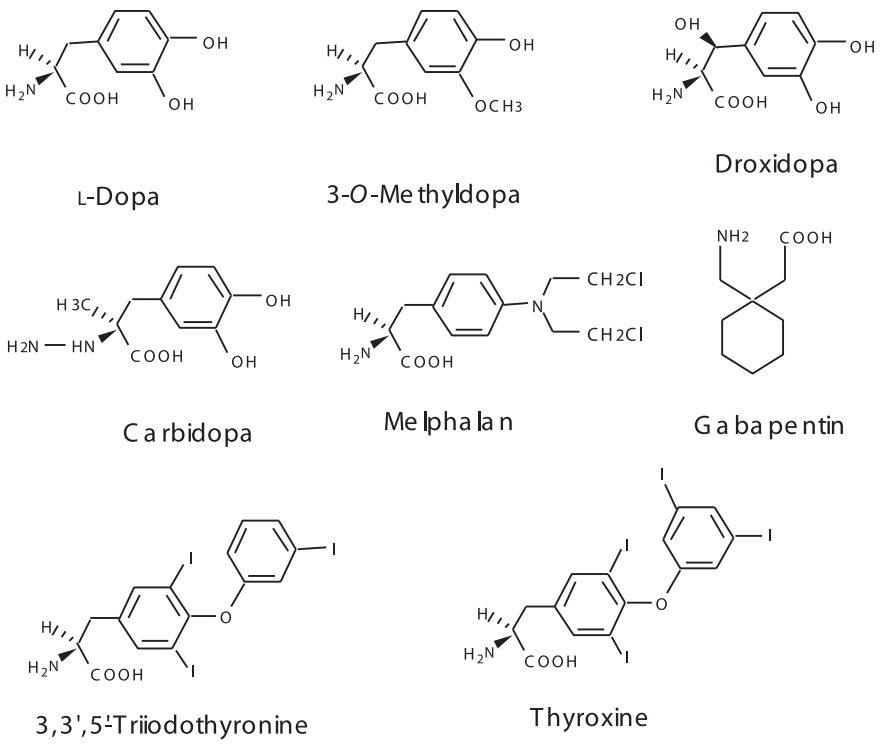

Fig. 1. Chemical structures of amino acid–related drugs used in the present study.

containing 0.05% trypsin–EDTA solution and used at passage 60 – 100 (29, 30). The full-length cDNAs for human L-type AA transporter 1 (hLAT1) (GenBank /EMBL/DDBJ accession no. AB018009) (4), and human L-type AA transporter 2 (hLAT2) (GenBank /EMBL/DDBJ accession no. AB037669) (27) were subcloned into pcDNA3.1; a mammalian expression vector (Invitrogen, San Diego, CA, USA) at KpnI /EcoRV and NotI restriction enzyme cleavage sites to obtain plasmids designated pcDNA3.1-hLAT1 and pcDNA3.1-hLAT2, respectively. The pcDNA3.1-hLAT1, pcDNA3.1-hLAT2, and pcDNA3.1 plasmid vector without insert were cotransfected with pSV2neo, a neomycin-resistance gene, into S2 cells using LIPOFECTAMIN 2000 regent (Invitrogen) according to the manufacturer's instructions (30). At 48 h after transfection, cells were subcultured in medium containing 400 μg/ml geneticin. The cell clones were isolated using a cloning cylinder (30). We obtained 17 colonies of S2-LAT1 and 21 colonies of S2-LAT2 cells and then we picked 11 and 12 colonies based on the RT-PCR experiment, respectively. Finally, we selected final clones that showed highest transport activities of [^{14}C]leucine. The cell clones transfected with pcDNA3.1 plasmid vector without insert were named S2-mock.

Reverse transcription polymerase chain reaction (RT-PCR)

Degenerate PCR primers were designed based on the AA sequences of hLAT1 (GenBank/EMBL/DDBJ accession no. AB018009), hLAT2 (GenBank/EMBL /DDBJ accession no. AB037669), mouse Lat1 (mLat1) (GenBank/EMBL/DDBJ accession number AB023409), mouse Lat2 (mLat2) (GenBank/EMBL/DDBJ accession number AF171668), and mouse 4F2hc (m4F2hc) (GenBank/EMBL/DDBJ accession number AB023408). The primers used in this experiment are indicated in Table 1. A 1-μg sample of total RNA prepared from S2-LAT1, S2-LAT2, and S2-mock cell lines using RNA purification kit ISOGEN (NIPPONGENE, Tokyo) was reverse-transcribed and used as a template for subsequent PCR with the set of degenerate primers (31). PCR was performed according to the following protocol: 94°C (30 s), 60°C (30 s), 72°C (60 s); 35 cycles. PCR products were subcloned in pCR II-TOPO vector using a TA cloning kit (Invitrogen) and sequenced by the dye terminator cycle sequencing method (Applied Biosystems, Foster City, CA, USA) (12).

Real-time quantitative RT-PCR

The 7700 Sequence Detector System (Applied Biosystems) was used for Real-time quantitative RT-PCR (32, 33). Briefly, each RT-PCR reaction mixture (50 μl) included 250 ng of total RNA, 25 μl of Taqman Universal PCR Master Mix (Applied Biosystems), 0.5 μl of forward and reverse primer (10 μM), and 1.0 μl of corresponding Taqman probe (5000 nM). RT-PCR cycle parameters were 50°C (2.0 min), 95°C (10.0 min), followed by 40 cycles at 95°C (15 s) and 60°C (60 s). The primers and probes were designed using Primer Express software (Applied Biosystems) and synthesized by Applied Biosystems. The sequences of primers used in this study are shown in Table 2. The concentrations of all primers and probes were optimized for LAT1; the concentrations of reverse and forward primers used for LAT1 were 900 nM. The LAT1 probe concentration was 250 nM.

Anti-peptide antibody generation

Oligopeptides [MAGAGPKRRALAAC] corresponding to AA residues 1 – 13 of hLAT1 and oligopeptides [EEANEDMEEQQQC] corresponding to AA residues 505 – 516 of hLAT2 were synthesized. The C-terminal cysteine residues were introduced for conjugation with keyhole limpet hemocyanine. Anti-peptide polyclonal antibodies were generated as described elsewhere (4).

Table 1. Summary of RT-PCR primers used in this study

Protein	Direction	Sequence (5' to 3')	Position
hLAT1	Forward	GCATGCGCAGAGGCCAGTTAA	1617–1637
	Reverse	TATGGTCAGGAGTCCATCGGG	2215–2235
hLAT2	Forward	TCCCCATCATACCTGCACCCA	2836–2856
	Reverse	TGCCCCAAGACAGCATGACAC	3527–3547
mLat1	Forward	GAGACCCTAGAGATGGAACCC	2154–2174
	Reverse	TCACATCACACTGGTGACAGAG	2569–2590
mLat2	Forward	GCCCATGGTCAAGGTCAATGC	2028–2048
	Reverse	GGCTTGGCTTCTGCAGTCTGA	2506–2526
m4F2hc	Forward	GAAGAACGGTCTGGTGAAGATC	194–215
	Reverse	CTGCAGGTCAGAGGACTCAGT	612–632

Table 2. Real-time RT-PCR primer sequences

Target		Sequence (5' to 3')
hLAT1	Forward	CCGCTGCACATGGACAGA
	Reverse	GTCCCTTGGACGAGTGGAATT
	TaqMan	6 FAM-AGCGTCTGCTCATAGGACCTGCATCC-TAMRA
hLAT2	Forward	GGTCTCAGTGTCATGCTGTCTTG
	Reverse	GAGGGCCTTTTTTGAGGATCTC
	TaqMan	6 FAM-AAAGGGTAGTGGCAGCAGGGCGC-TAMRA
mLat1	Forward	CTACTGTGTGGGTCACTTGTTAGGTT
	Reverse	TCCATATGGAGCCAGGACTTCA
	TaqMan	6 FAM-AAATTTAGAGCTCAGCTCTCGCCGCC-TAMRA
mLat2	Forward	CCCAGCAATAGCTAGGAAGACAA
	Reverse	GGAGAATGAAGCCACATCTGAGTA
	TaqMan	6 FAM-TCAGATTGTCACCGTTAAGTCAGCTGGAGA-TAMRA
m4F2hc	Forward	GAAGAACGGTCTGGTGAAGATCA
	Reverse	TGGATAAGCCGGTGAACTTGA
	TaqMan	6 FAM-TGGCGGAGGACGAGACGGAGG-TAMRA

Antisera were affinity-purified as described elsewhere (4).

Western blot analysis

Cell membranes of S2-mock cells, S2-LAT1 cells, and S2-LAT2 cells as well as T24 human bladder carcinoma cells were prepared as described elsewhere (19), with minor modifications. Briefly, these cells were homogenized in 9 vol. of a solution containing 50 mM Tris-HCl (pH 7.5), 25 mM KCl, 1 mM $MgCl_2$, 1 mM phenylmethylsulfonyl fluoride, and 0.25 M sucrose, with 15 strokes in a Dounce homogenizer. The homogenate was centrifuged for 10 min at $8,000 \times g$, and the supernatant was centrifuged further for 1 h at $100,000 \times g$. After centrifugation, the membrane pellet was resuspended in a solution containing 0.25 M sucrose, 100 mM KCl, 5 mM $MgCl_2$, and 50 mM Tris (pH 7.4). The protein samples were heated at 100°C for 5 min in the sample buffer either in the presence (reducing condition) or absence (nonreducing condition) of 5% 2-mercaptoethanol and then subjected to SDS-polyacrylamide gel electrophoresis. The separated proteins were transferred electrophoretically to a Hybond-P PVDF transfer membrane (Amersham Pharmacia Biotech, Uppsala, Sweden) that was then treated with nonfat dried milk and an affinity-purified anti-hLAT1 antibody (1:500 dilution) or anti-hLAT2 antiserum (1:1,000 dilution). The membrane was then treated with horseradish-peroxidase–conjugated anti-rabbit IgG as the secondary antibody (Jackson ImmunoResearch Laboratories, Inc., West Grove, PA, USA). The signals were detected using an ECL plus system (Amersham Pharmacia Biotech) (19).

Immunoprecipitation

S2-LAT1 and S2-LAT2 cells were lysed with a lysis buffer (1% Nonidet P-40, 50 mM Tris-Cl, pH 7.4, 0.15 M NaCl, 10 mM EDTA, PMSF, leupeptin, antipain, chymostatin trypsin inhibitor) and incubated with anti-mouse 4F2hc antibody (5 μl) (BD Bioscience, San Jose, CA, USA) and protein A-Sepharose 4B (Amersham Pharmacia Biotech) at 4°C for 2 h. The protein samples were electrophoresed in SDS-PAGE. Western blot analysis was done as described above. The anti-hLAT1 antibody and the anti-hLAT2 antibody were used to detect hLAT1 and hLAT2, respectively. In the absorption experiments, the membranes were treated with primary antibodies in the presence of antigen peptides (100 μg/ml) (4).

Uptake measurement

For AA uptake measurements, S2-LAT1, S2-LAT2, and S2-mock cells were used two days after plating (90% – 100% confluence) on 24-well plates (30). After removal of the medium, the cells were washed twice with Hank's Na^+ free buffer (125 mM choline chloride, 4.8 mM KCl, 1.3 mM $CaCl_2$, 1.2 mM $MgCl_2$, 25.0 mM HEPES, and 5.0 mM Tris, pH 7.4) supplemented with D-glucose (5.6 mM) and preincubated for 10 min (37°C). Thereafter, cells were incubated (1.0 min, 37°C) with uptake medium (500 μl of Hank's Na^+-free buffer) containing [^{14}C]L-leucine. The cells were washed three times with medium and solubilized with 0.1 N NaOH (500 μl). Substrate accumulation was then measured by counting radioactivity by liquid scintillation counting (LSC; LSC6100, Aloka, Tokyo) (20, 34).

For the inhibition experiments, unless otherwise

indicated, [^{14}C]L-leucine uptake (10 μM) by S2-LAT1, S2-LAT2, or S2-mock cells was measured in the presence or absence of 1.0 mM non-labeled test compounds. For T3, T4, and melphalan, the effects of non-radiolabeled compounds were examined on the uptake of 1.0 μM [^{14}C]L-leucine in the uptake solution containing a final concentration of 1.0% DMSO (4).

The AA substrate K_m and V_{max} values were determined using the Eadie-Hofstee equation based on the LAT1- and LAT2-mediated AA uptakes measured for 60 s at 3.0, 10, 30, 100, 300, 1000, and 2000 μM. The LAT1- and LAT2-mediated AA uptakes were calculated as the differences between the means of uptakes from cDNA-transfected cells and those of mock-transfected controls.

To determine K_i values, S2-LAT1, S2-LAT2, and S2-mock cells were incubated (60 s) in uptake solution with different [^{14}C]L-leucine concentrations with or without inhibitor. The K_i values were determined by double-reciprocal–plot analysis where 1/[^{14}C]L-leucine uptake rate was plotted against 1/[^{14}C]L-leucine concentration. When competitive inhibition was observed, K_i values were calculated from the following equation: K_i = concentration of inhibitor / [(Leucine K_m with inhibitor / Leucine K_m without inhibitor) − 1] (4, 35).

Statistical analyses

Values are presented as means ± S.E.M. (n = 6 – 8). Statistical differences were analyzed by Student's unpaired *t*-test.

Results

Expression of hLAT1 and hLAT2 in cell lines

Exogenous hLAT1 and hLAT2 expression in S2-LAT1 and S2-LAT2 cells was examined via agarose gel electrophoresis (Fig. 2A). Consistent with levels observed in S2-mock cells, S2-LAT1 and S2-LAT2 cell lines expressed endogenous mLat1, mLat2, and m4F2hc. Furthermore, significant levels of exogenous hLAT1 and hLAT2 expression were quantitatively determined; they were performed to compare endogenous mLat1, mLat2, and m4F2hc using real-time quantitative RT-PCR from S2-LAT1 and S2-LAT2 cells, respectively (Fig. 2B). In S2-LAT1 cells, hLAT1 was detected as well as endogenous mLat1, mLat2, and m4F2hc; hLAT1 was 21-fold higher than mLat1 and >1000-fold higher than mLat2. Likewise, in S2-LAT2 cells, hLAT2 was detected as well as mock levels of endogenous mLat1, mLat2, and m4F2hc; however, hLAT2 was 86-fold higher than mLat1 and >200-fold higher than mLat2. Furthermore, hLAT1 was 2.1-fold higher than m4F2hc in S2-LAT1 cells, while hLAT2 was 8.4-fold higher than m4F2hc in S2-LAT2 cells. In S2-mock cells, hLAT1 and hLAT2 were not detected and the amount of mLat1 was 59-fold higher than that of mLat2.

Western blot analysis was performed on the membrane fractions prepared from S2-Mock cells, S2-LAT1 cells, and S2-LAT2 cells as well as T24 human bladder carcinoma cells. The antibodies raised against AA sequences of human LAT1 and LAT2, which are less conserved with mouse sequences, were used to detect exogenously expressed human LAT1 and LAT2 in S2 cells. The anti-hLAT1 antibody recognized the 125 kDa–protein band under the nonreducing condition, whereas this band shifted to the 38 kD–protein band for hLAT1 in the S2-LAT1 cells (Fig. 2C). The size was consistent with the 38 kDa–protein band in the T24 cells (36). The antibodies raised against hLAT2 recognized the 130 kDa–protein band under the nonreducing condition, whereas this band shifted to the 45 kDa–protein band for hLAT2 in the S2-LAT2 cells (Fig. 2C).

To confirm the endogenous 4F2hc in S2 cells coupled with exogenously expressed hLAT1 and hLAT2, we conducted co-immunoprecipitation experiments in which an anti-mouse 4F2hc antibody was used to detect mouse 4F2hc-hLAT1 and mouse 4F2hc-hLAT2 complexes in S2-hLAT1 cells and S2-hLAT2 cells, respectively. The hLAT1 and hLAT2 in the immunoprecipitate were detected by antibodies raised against AA sequences of human LAT1 and LAT2, which are less conserved with mouse sequences. As shown in Fig. 2D, the anti-mouse 4F2hc antibody immunoprecipitated human LAT1 in S2-LAT1 cell membrane. A 37-kDa band was visible under reducing conditions. This band disappeared in the absorption experiment, confirming it as the band for hLAT1. In S2-LAT2 cells, a 45-kDa band was detected by anti-hLAT2 antibody under the reducing condition. The absorption test confirmed it as hLAT2.

Transport activity

To directly compare the transport rates of hLAT1 and hLAT2, we performed uptake studies of [^{14}C]L-leucine (10 μM) using S2-mock, S2-LAT1, and S2-LAT2 cells. As shown in Fig. 2, S2-LAT1 and S2-LAT2 cells exhibited significantly higher L-leucine uptake than S2-mock cells (uptake by the endogenous transporter). Then we analyzed transport properties of S2-LAT1 and S2-LAT2 cells.

As presented in Fig. 3A, [^{14}C]L-leucine (10 μM) uptake mediated by S2-LAT2 cells was time-dependent and exhibited a linear dependence during the first 2 – 3 min. The [^{14}C]L-leucine uptake by S2-LAT1 cells also exhibited a similar dependence on incubation time (data not shown). Thus, all subsequent uptake measurements were conducted for 1.0 min and data expressed

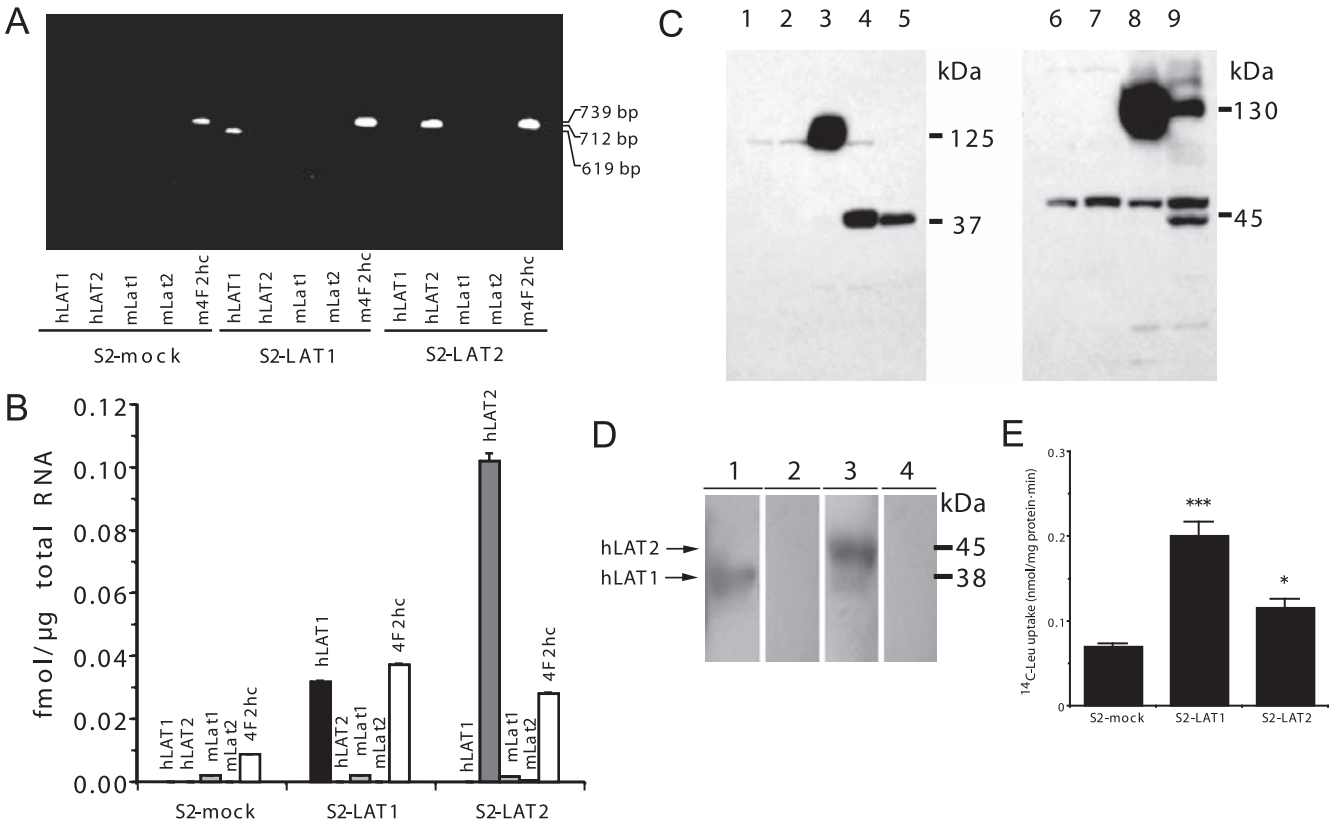

Fig. 2. hLAT1 and hLAT2 expression in S2-LAT1 and S2-LAT2 cells. A: Agarose gel electrophoresis showing hLAT1, hLAT2, mLat1, mLat2, and m4F2hc RT-PCR products in S2-mock, S2-LAT1, and S2-LAT2 cells. B: Real-time PCR analysis of mRNA expression for hLAT1, hLAT2, mLat1, mLat2, and m4F2hc in S2-mock, S2-LAT1, and S2-LAT2 cells. C: Western blot analysis was performed on the membrane fraction prepared from S2-mock, S2-LAT1, S2-LAT2, and T24 cells in the presence or absence of 2-mercaptoethanol using antibodies for hLAT1 and hLAT2. Anti-hLAT1 antibody did not react with S2-mock cells in the absence (lane 1) or presence (lane 2) of 2-mercaptoethanol (2-ME). The 125 kDa–protein band detected in the absence of 2-ME in the S2-LAT1 cells (lane 3) was shifted to a 38 kDa–protein band in the presence 2-ME (lane 4). A 38 kDa–protein band was detected in the presence 2-ME in T24 cells (lane 5). Anti-hLAT2 antibody did not react with S2-mock cells in the absence (lane 6) or presence (lane 7) of 2-ME. The 130 kDa–protein band detected in the absence of 2-ME in the S2-LAT2 cells (lane 8) was shifted to a 45 kDa–protein band in the presence 2-ME (lane 9). D: Immunoprecipitation was conducted on S2-LAT1 cells (lanes 1 and 2) and S2-LAT2 cells (lanes 3and 4) using anti-mouse 4F2hc antibody. In S2-LAT1 cells, hLAT1 in the immunoprecipitant was detected by an anti-hLAT1 antibody (lane 1) in the reducing condition. The band disappeared in the presence of an antigen peptide in the absorption experiment (lane 2). In S2-LAT2 cells, hLAT2 in the immunoprecipitant was detected by an anti-hLAT2 antibody (lane 3) in the reducing condition, but this disappeared in the presence of an antigen peptide (lane 4). E: Comparison of [^{14}C]L-leucine (10 μM) uptake for 1 min by S2-mock, S2-LAT1, and S2-LAT2 cells. *P<0.05, ***P<0.001 *vs* S2-mock.

as nmol/mg protein·min. The [^{14}C]L-leucine uptake by S2-LAT1 cells and S2-LAT2 cells was saturable and followed Michaelis-Menten kinetics (Fig. 3B for S2-LAT2 cells). The K_m values were 80.3 ± 9.7 and 318.0 ± 4.0 μM and the V_{max} values were 16.2 ± 2.9 and 31.2 ± 3.9 ng/mg protein·min (mean ± S.E.M. of 3 measurements), respectively.

Inhibition of [^{14}C]L-leucine uptake by L- and D-AAs

[^{14}C]L-leucine (10 μM) uptake was measured in the presence of 1.0 mM nonlabeled L- or D-AAs. As summarized in Fig. 4, A and B, [^{14}C]L-leucine uptake by S2-mock cells and S2-LAT1 cells was highly inhibited by the L-isomers of leucine, isoleucine, valine, phenylalanine, tyrosine, tryptophan, methionine, and histidine and a classical SL specific inhibitor, 2-aminobicyclo-(2,2,1)-heptane-2-carboxylic acid (BCH). L-Isomers of alanine, serine, threonine, cysteine, asparagines, and glutamine exhibited weaker but significant inhibition on [^{14}C]L-leucine uptake by S2-LAT1 cells (Fig. 4B), whereas weaker inhibition was detected for L-threonine and L-cysteine by S2-mock cells (Fig. 4A). Proline, glycine, cystine, basic AAs such as lysine and arginine, and acidic AAs such as glutamate and aspartate did not inhibit [^{14}C]L-leucine uptake by S2-mock and S2-LAT1 cells (Fig. 4: A and B); with the exception of glycine, the same general non-inhibition was observed in S2-LAT2 cells (Fig. 4C). In S2-LAT2 cells, [^{14}C]L-leucine uptake

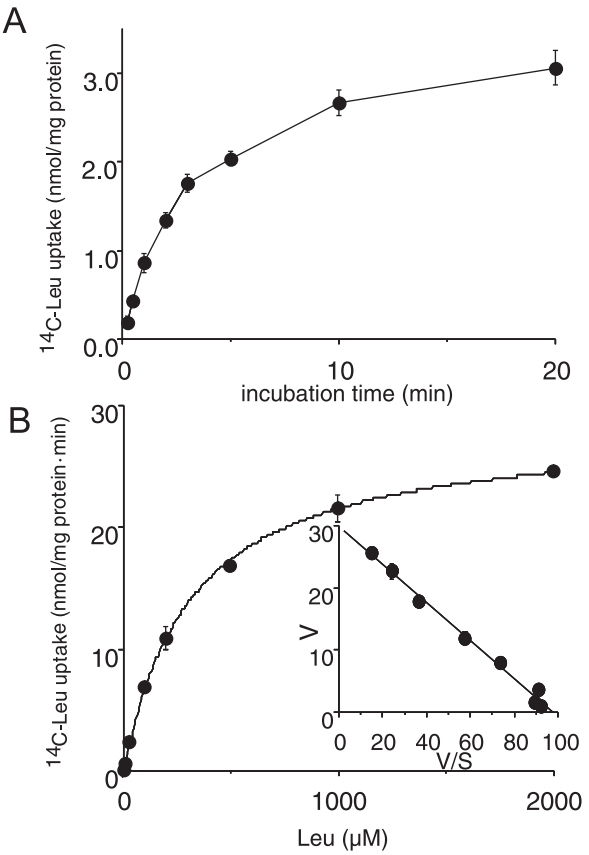

Fig. 3. [^{14}C]L-Leucine uptake by S2-LAT2 cells. A: Time course of [^{14}C]L-leucine (10 μM) uptake by S2-LAT2 cells. B: [^{14}C]L-Leucine concentration (3, 10, 20, 50, 100, 300, 1000, and 2000 μM)-dependent uptake measured in S2-LAT2 cells and plotted against L-leucine concentration. L-Leucine uptake was saturable and fit to the Michaelis-Menten equation. The inset shows the L-leucine uptake Eadie-Hofstee plot used to determine the kinetic parameters.

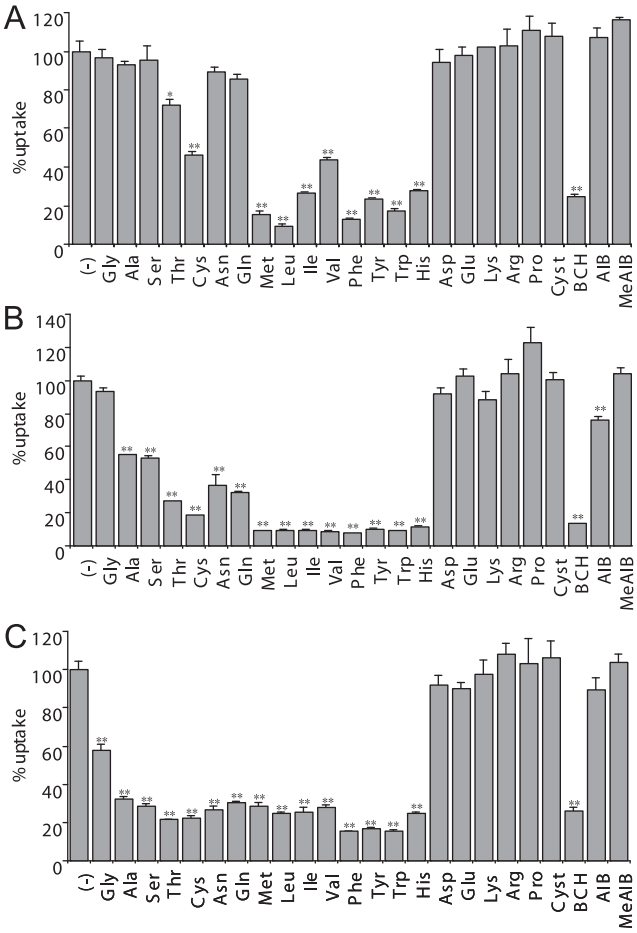

Fig. 4. [^{14}C]L-Leucine uptake inhibition by glycine and L-amino acids. The uptake of [^{14}C]L-leucine (10 μM) was measured in the presence of 1.0 mM nonradiolabeled glycine and indicated L-amino acids for S2-mock (A), S2-LAT1 (B), and S2-LAT2 cells (C). The values are expressed as percent of the [^{14}C]L-leucine uptake control measured in the absence of inhibitors. Cyst, L-cystine; AIB, α-aminoisobutyric acid; MeAIB, α-(methylamino)isobutyric acid. *P<0.05, **P<0.01 *vs* control.

was strongly inhibited by L-isomers of AAs containing apolar and uncharged polar groups (except proline), histidine, glycine (moderate inhibition), and BCH (Fig. 4C).

D-Isomers of methionine, leucine, and phenylalanine strongly inhibited [^{14}C]L-leucine uptake by S2-mock and S2-LAT1 cells (Fig. 5: A and B); weak inhibition was detected with D-tyrosine in S2-mock cells. D-Isomers of isoleucine, tyrosine, histidine, cysteine, asparagine, and glutamine exhibited weaker but statistically significant inhibition of [^{14}C]L-leucine uptake by S2-LAT1 cells (Fig. 5B). In S2-LAT2 cells, [^{14}C]L-leucine uptake was weakly inhibited by D-isomers of phenylalanine, tyrosine, asparagine, methionine, leucine, isoleucine, and valine (Fig. 5C).

Inhibition of [^{14}C]L-leucine uptake by AA-related compounds

[^{14}C]L-Leucine (10 μM) uptake was measured in the presence of 1.0 mM nonlabeled AA-related compounds. As summarized in Fig. 6A, [^{14}C]L-leucine uptake by S2-LAT1 cells was markedly inhibited by L-dopa, 3-*O*-methyldopa, α-methylphenylalanine, α-methyltyrosine, α-methyldopa, and gabapentin; phenylalanine methylester exhibited weak inhibition. In S2-LAT2 cells (Fig. 6B), [^{14}C]L-leucine uptake was strongly inhibited by L-dopa and 3-*O*-methyldopa, while α-methylphenylalanine, α-methyltyrosine, α-methyldopa, phenylalanine methylester, and gabapentin caused weak or no inhibition.

In addition, AA-related compounds (10 μM) with bulky side chains (i.e., melphalan, T3, and T4) were also examined (Fig. 7: A and 7B). [^{14}C]L-Leucine uptake by S2-LAT1 cells (Fig. 7A) was markedly inhibited by T3, whereas T4 was weakly inhibitory, and melphalan was

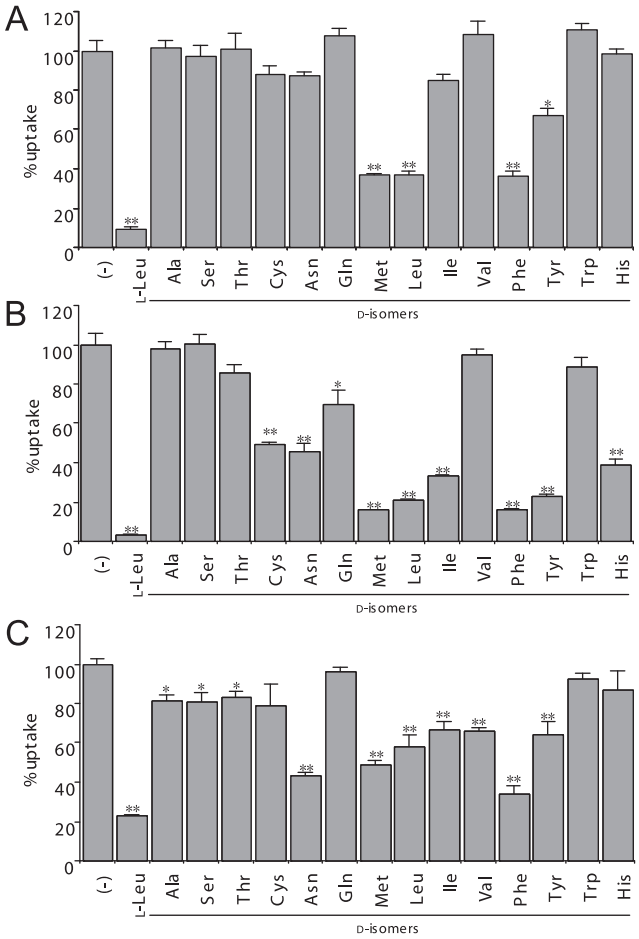

Fig. 5. [^{14}C]L-Leucine uptake inhibition by D-amino acids. [^{14}C]L-Leucine (10 μM) uptake was measured in the presence of 1.0 mM nonradiolabeled D-amino acids for S2-mock (A), S2-LAT1 (B), and S2-LAT2 (C) cells. The values are expressed as percent of the [^{14}C]L-leucine uptake control measured in the absence of inhibitors. **P*<0.05, ***P*<0.01 *vs* control.

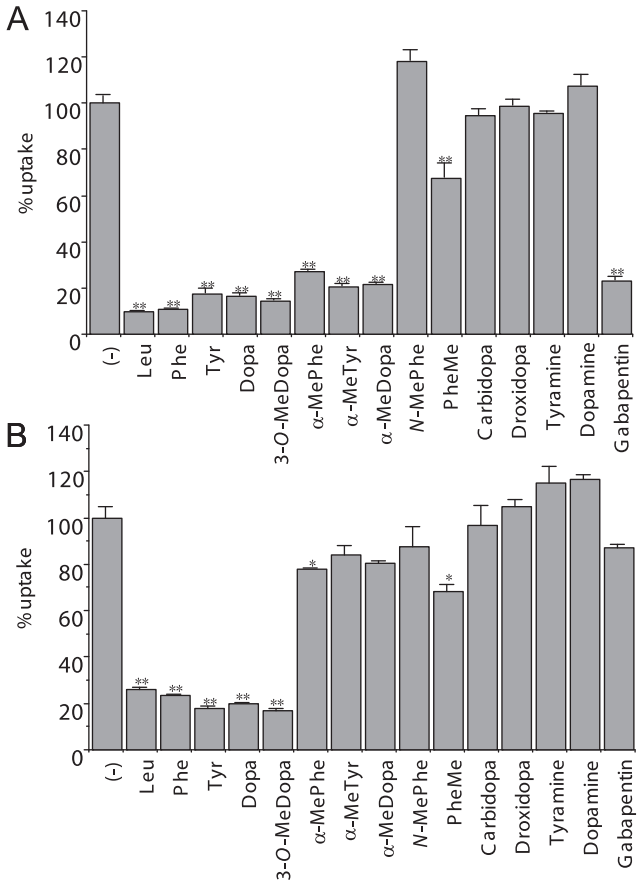

Fig. 6. [^{14}C]L-Leucine uptake inhibition by amino acid–related compounds. [^{14}C]L-Leucine (10 μM) uptake was measured in the absence (–) or presence of 1.0 mM non-radiolabeled L-leucine (Leu), L-phenylalanine (Phe), L-tyrosine (Tyr), L-dopa, 3-*O*-methyldopa (3-*O*-MeDopa), α-methylphenylalanine (α-MePhe), α-methyltyrosine (α-MeTyr), α-methyldopa (α-MeDopa), *N*-methylphenylalanine (*N*-MePhe), phenylalanine methylester (Phe-Me), carbidopa, droxidopa, tyramine, dopamine, and gabapentin for S2-LAT1 (A) and S2-LAT2 cells (B). The uptake values are expressed as percent of the [^{14}C]L-leucine uptake control measured in the absence of inhibitors (–). **P*<0.05, ***P*<0.01 *vs* control.

not inhibitory. In S2-LAT2 cells (Fig. 7B), T3 and T4 were weak inhibitors of [^{14}C]L-leucine uptake, while melphalan was not inhibitory. Furthermore, concentration-dependent [^{14}C]L-leucine uptake inhibition was further probed, and the obtained K_i values for BCH, T3, T4, and melphalan are summarized in Tables 3 and 4.

Discussion

Mouse cell lines S2-LAT1 and S2-LAT2 stably expressing hLAT1 and hLAT2 at high levels via hLAT1 and hLAT2 cDNA transfection have been established. The real-time quantitative RT-PCR analysis illustrated that exogenously introduced hLAT1 and hLAT2 levels were 20 – 1000-fold higher than endogenous mLat1 and mLat2 levels in S2-LAT1 cells and S2-LAT2 cells (Fig. 2B). In addition, hLAT1 and hLAT2 levels were 2 – 8-fold higher than endogenous m4F2hc. Hence, due to the high levels of hLAT1 and hLAT2 expression, one may predict that endogenous m4F2hc is associated with hLAT1 and hLAT2 in the S2-LAT1 and S2-LAT2 cells, respectively. As illustrated from the present Structure Activity Relationship (SAR) studies probing [^{14}C]L-leucine transport, the transport function of these stably transfected S2 cell lines reflect the properties of exogenously introduced hLAT1 and hLAT2.

In S2-mock cells, [^{14}C]L-leucine uptake inhibition data by L- and D-AAs (Figs. 4 and 5) are consistent with results observed using the *Xenopus* oocyte expression system (4, 11). The real-time quantitative RT-PCR analysis results indicate that mLat1 was expressed at higher levels than mLat2 (Fig. 2B). Furthermore, [^{14}C]L-

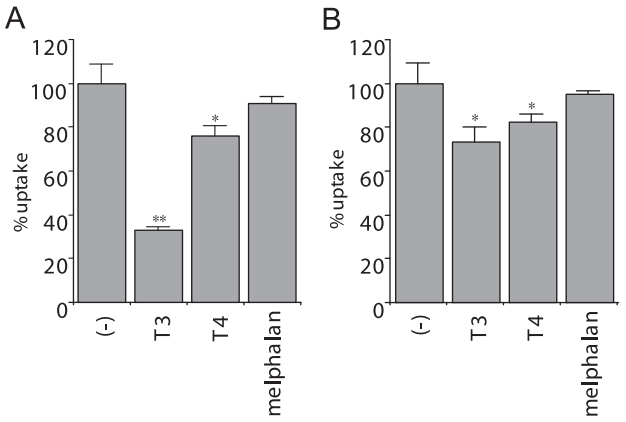

Fig. 7. [^{14}C]L-Leucine uptake inhibition by amino acids and related compounds. [^{14}C]L-Leucine (1.0 μM) was measured in the absence (–) or presence of 10 μM non-radiolabeled triiodothyronine (T3), thyroxine (T4), and melphalan for S2-LAT1 (A) and S2-LAT2 cells (B). The uptake values are expressed as percent of the [^{14}C]L-leucine uptake control measured in the absence of inhibitors (–). *P<0.05, **P<0.01 *vs* control.

Table 3. Kinetic parameters of amino acid–related compounds in S2-LAT1 cells

Compounds	K_i (μM)	K_m (μM)
Leucine	114.0 ± 8.3	80.3 ± 9.7
BCH	132.0 ± 27.8	
Melphalan	205.0 ± 32.0	
T3	1.7 ± 0.1	
T4	115.0 ± 2.0	

Table 4. Kinetic parameters of amino acid-related compounds in S2-LAT2 cells

Compounds	K_i (μM)	K_m (μM)
Leucine	480.0 ± 19.4	318.0 ± 4.0
BCH	315.0 ± 68.6	

leucine uptake inhibition by L- and D-amino acids in S2-LAT1 cells are fairly consistent with results observed via hLAT1-expressing *Xenopus* oocytes (4, 11); L-alanine, L-serine, D-tyrosine, D-histidine, D-cysteine, D-asparagine, and D-glutamine exhibited higher levels of inhibition in S2-LAT1 cells (Fig. 4B and 5B). In S2-LAT2 cells (Fig. 4C), [^{14}C]L-leucine uptake was inhibited by neutral AAs – apolar and uncharged polar groups, except proline – and in agreement with the transport properties of LAT2 examined in hLAT2-expressing *Xenopus* oocytes (12, 27, 28). Also consistent with the properties of hLAT2-expressing oocytes, [^{14}C]L-leucine uptake by S2-LAT2 cells was weakly inhibited by D-asparagine and D-phenylalanine (12) (Fig. 5C). Therefore, the inhibition experiments using L- and D-AAs indicate that [^{14}C]L-leucine uptake in S2-LAT1 and S2-LAT2 cells reflect the properties of exogenously introduced hLAT1 and hLAT2, respectively.

Exogenously introduced hLAT1 and hLAT2 in S2-LAT1 and S2-LAT2 cells, respectively, are presumed to be linked with endogenous m4F2hc. The functional expression and role of 4F2hc in heterodimeric AA transporters is well established; 4F2hc promotes the trafficking of the associating transporter proteins to the plasma membrane (3, 20, 37). However, it is important to point out that 4F2hc appears to not contribute to the assembly of transporter substrate binding sites; a fusion protein of LAT1 and 4F2hc and that of LAT1 and the other single membrane spanning heavy chain rBAT (related to $b^{0,+}$ AA transporter) have exhibited similar substrate selectivity and affinity (20). Furthermore, hLAT1 and human 4F2hc coexpression and hLAT1 and mouse 4F2hc coexpression in *Xenopus* oocytes resulted in similar substrate selectivity and affinity (data not shown). Hence, L-leucine transport detected in the absence of Na^+ in S2-LAT1 and S2-LAT2 cells reflects the inherent properties of hLAT1 and hLAT2; cells that may mimic transport mediated by hLAT1 and hLAT2 in vivo and affords novel in vitro screening tools.

Using S2-LAT1 and S2-LAT2 cells, we have examined the SAR of hLAT1 and hLAT2 expressed in mammalian cells. As illustrated in Fig. 6, A and B, *N*-methyl-phenylalanine had little effect on [^{14}C]L-leucine uptake in both S2-LAT1 and S2-LAT2 cells, which is consistent with previous data from inhibition studies on rLat1-expressing oocytes (38). Thus, the α-amino group appears essential for substrate-binding by hLAT1 and hLAT2. In agreement, tyramine and dopamine, which both lack α-carboxyl groups, and carbidopa, an *N*-amino derivative of L-α-methyldopa (Fig. 1), failed to inhibit [^{14}C]L-leucine uptake in S2-LAT1 and S2-LAT2 cells (Fig. 6: A and B). These results are in contrast to the system T transporter TAT1 that recognizes aromatic AA substrates as anions (39). All compounds that efficiently inhibited [^{14}C]L-leucine uptake in S2-LAT1 and S2-LAT2 cells were α-AAs, except gabapentin (a γ-AA), and inhibited hLAT1-mediated [^{14}C]L-leucine uptake but not hLAT2-mediated uptake (Fig. 6: A and B).

It is interesting that hLAT1 accepts α-methyl AA while hLAT2 does not (Fig. 6: A and B). L-α-Methyl-phenylalanine, L-α-methyltyrosine, and L-α-methyldopa inhibited hLAT1-mediated [^{14}C]L-leucine uptake but not hLAT2-mediated uptake, which indicates that the binding site of hLAT1, but not hLAT2, can accommodate methyl substituents on the α-carbon. Therefore, the substrate binding site on hLAT1 seems to have more space around the α-carbon–binding region compared to

hLAT2. Also consistent with a more rigid hLAT2 binding site, hLAT1 accepts gabapentin while hLAT2 does not (Fig. 6: A and B); this situation enables hLAT2 to exclude α-methyl AA and the γ-AA gabapentin.

Consistent with the observations on SL in cultured cells or membrane-vesicle preparations, hLAT1-mediated transport is inhibited by thyroid hormones (i.e., T3 and T4) and by melphalan (Fig. 7A) (6 – 8, 40, 41). It was previously reported that IU12/ASUR4, a *Xenopus* homolog of LAT1, accepts thyroid hormones as substrates (42); based on the double-reciprocal-plot analysis (data not shown), these modified AAs with bulky side chains are determined to be competitive inhibitors of hLAT1-mediated transport. Therefore, hLAT1's binding site may accommodate bulky side chains such as those of the thyroid hormones and melphalan. In contrast, hLAT2-mediated transport is inhibited markedly by thyroid hormones and melphalan (Fig. 7B). Consequently, hLAT1's substrate binding site appears to contain a larger pocket (and/or more flexible pocket) that may accept the bulky side chains of thyroid hormones and melphalan. On the other hand, hLAT2 compared to hLAT1, exhibits a broader substrate selectivity for common neutral AAs.

In the present study, we have established mouse cell lines stably expressing human SL transporters hLAT1 and hLAT2 and demonstrate that these cell lines are quite useful for evaluating the interaction of chemical compounds with hLAT1 and hLAT2. SL is a major route through which living cells take up neutral AAs from extracellular fluids (1). It was shown that LAT1 is upregulated in tumor cells to provide tumor cells with AAs to support their continuous growth and proliferation (1, 3, 4, 21, 22). In addition, LAT1 is proposed to mediate the permeation of AAs through blood-tissue barriers such as the BBB and PB (23 – 26). In contrast, LAT2 may be regarded as the "normal cell type" transporter essential for AA transport in cells and important in epithelial transport of AAs in the small intestine and kidney (3, 12, 28). Therefore, the development of isoform specific inhibitors or substrates should have important therapeutic implications (3). For example, LAT1-selective inhibitors may be useful as anti-tumor agents with less side effects on non-tumor cells; selectively inhibiting LAT1 predominantly expressed in tumor cells may sufficiently suppress tumor cell growth by reducing the AA supply to tumor cells (3, 43, 44) – an "AA starve-out strategy". Although it is not LAT1-specific, a new class of immunosuppressant, brasilicardin A (BraA), has been found to be an inhibitor of the AA transporter SL (45). Usui et al. suggested that the immunosuppressive activity of BraA is induced by AA deprivation via the inhibition of SL and that the AA transporter is a target for the immunosuppressant (45).

Another application of LAT1-selective compounds may be for diagnostic usage; such compounds can be specifically designed to target cancer cells via LAT1 interactions at blood–tissue barriers (3). Anti-tumor agents designed to be transported by LAT1 are expected to be selectively taken up and accumulate in tumor cells. Recently, Kaira et al. evaluated the diagnostic usefulness of L-[3-^{18}F]-α-methyltyrosine ([^{18}F]FMT), an AA tracer for positron emission tomography (PET), in non-small-cell lung cancer (NSCLC) patients (46). In that study, they compared [^{18}F]FMT to 2-[^{18}F]-fluoro-2-deoxy-D-glucose ([^{18}F]FDG) tumor uptake and correlated the results with LAT1 expression. They found that [^{18}F]FMT PET had no false-positives in primary tumor and lymph node metastasis detection and could improve NSCLC diagnostic performance. In addition, [^{18}F]FMT uptake correlated with LAT1 expression and showed a significant association with cellular proliferation (45). Therefore, by having more robust in vitro tools for high-throughput compound screening, S2-LAT1 and S2-LAT2 cell lines established in the present study are expected to contribute to the development of novel anti-cancer and diagnostic agents.

Acknowledgments

This work was supported in part by grants from the Ministry of Education, Culture, Sports, Science, and Technology of Japan; the Japan Society for the Promotion of Science; the Promotion and Mutual Aid Corporation for Private Schools of Japan; Japan Foundation for Applied Enzymology; and the Japan Health Sciences Foundation. The authors are grateful to Michi Takahashi for technical assistance.

References

1 Christensen HN. Role of amino acid transport and countertransport in nutrition and metabolism. Physiol Rev. 1990;70:43–77.
2 Oxender DL, Christensen HN. Evidence for two types of mediation of neutral and amino-acid transport in Ehrlich cells. Nature. 1963;197:765–767.
3 Kanai Y, Endou H. Heterodimeric amino acid transporters: molecular biology and pathological and pharmacological relevance. Curr Drug Metab. 2001;2:339–354.
4 Yanagida O, Kanai Y, Chairoungdua A, Kim DK, Segawa H, Nii T, et al. Human L-type amino acid transporter 1 (LAT1): characterization of function and expression in tumor cell lines. Biochim Biophys Acta. 2001;1514:291–302.
5 Gomes P, Soares-da-Silva P. L-DOPA transport properties in an immortalised cell line of rat capillary cerebral endothelial cells, RBE 4. Brain Res. 1999;829:143–150.
6 Goldenberg GJ, Lam HY, Begleiter A. Active carrier-mediated

transport of melphalan by two separate amino acid transport systems in LPC-1 plasmacytoma cells in vitro. J Biol Chem. 1979;254:1057–1064.
7 Lakshmanan M, Goncalves E, Lessly G, Foti D, Robbins J. The transport of thyroxine into mouse neuroblastoma cells, NB41A3: the effect of L-system amino acids. Endocrinology. 1990;126: 3245–3250.
8 Blondeau JP, Beslin A, Chantoux F, Francon J. Triiodothyronine is a high-affinity inhibitor of amino acid transport system L1 in cultured astrocytes. J Neurochem. 1993;60:1407–1413.
9 Su TZ, Lunney E, Campbell G, Oxender DL. Transport of gabapentin, a gamma-amino acid drug, by system l alpha-amino acid transporters: a comparative study in astrocytes, synaptosomes, and CHO cells. J Neurochem. 1995;64:2125–2131.
10 Patel NJ, Fullone JS, Anders MW. Brain uptake of S-(1,2-dichlorovinyl)glutathione and S-(1,2-dichlorovinyl)-L-cysteine, the glutathione and cysteine S-conjugates of the neurotoxin dichloroacetylene. Brain Res Mol Brain Res. 1993;17:53–58.
11 Kanai Y, Segawa H, Miyamoto K, Uchino H, Takeda E, Endou H. Expression cloning and characterization of a transporter for large neutral amino acids activated by the heavy chain of 4F2 antigen (CD98). J Biol Chem. 1998;273:23629–23632.
12 Segawa H, Fukasawa Y, Miyamoto K, Takeda E, Endou H, Kanai Y. Identification and functional characterization of a Na^+-independent neutral amino acid transporter with broad substrate selectivity. J Biol Chem. 1999;274:19745–19751.
13 Babu E, Kanai Y, Chairoungdua A, Kim DK, Iribe Y, Tangtrongsup S, et al. Identification of a novel system L amino acid transporter structurally distinct from heterodimeric amino acid transporters. J Biol Chem. 2003;278:43838–43845.
14 Bodoy S, Martin L, Zorzano A, Palacin M, Estevez R, Bertran J. Identification of LAT4, a novel amino acid transporter with system L activity. J Biol Chem. 2005;280:12002–12011.
15 Verrey F, Jack DL, Paulsen IT, Saier Jr. MH, Pfeiffer R. New glycoprotein-associated amino acid transporters. J Membrane Biol. 1999;172:181–192.
16 Fukasawa Y, Segawa H, Kim JY, Chairoungdua A, Kim DK, Matsuo H, et al. Identification and characterization of a Na^+-independent neutral amino acid transporter that associates with the 4F2 heavy chain and exhibits substrate selectivity for small neutral D- and L-amino acids. J Biol Chem. 2000;275:9690–9698.
17 Torrents D, Estevez R, Pineda M, Fernandez E, Lloberas J, Shi Y-B, et al. Identification and characterization of a membrane protein (y^+L amino acid transporter-1) that associates with 4F2hc to encode the amino acid transport activity y^+L. A candidate gene for lysinuric protein intolerance. J Biol Chem. 1998;273: 32437–32445.
18 Sato H, Tamba M, Ishii T, Bannai S. Cloning and expression of a plasma membrane cystine/glutamate exchange transporter composed of two distinct proteins. J Biol Chem. 1999;274: 11455–11458.
19 Chairoungdua A, Segawa H, Kim JY, Miyamoto K, Haga H, Fukui Y, et al. Identification of an amino acid transporter associated with the cystinuria-related type II membrane glycoprotein. J Biol Chem. 1999;274:28845–28848.
20 Chairoungdua A, Kanai Y, Matsuo H, Inatomi J, Kim DK, Endou H. Identification and characterization of a novel member of the heterodimeric amino acid transporter family presumed to be associated with an unknown heavy chain. J Biol Chem. 2001; 276:49390–49399.
21 Sang J, Lim Y-P, Panzica M, Finch P, Thompson NL. TA1, a highly conserved oncofetal complementary DNA from rat hepatoma, encodes an integral membrane protein associated with liver development, carcinogenesis, and cell activation. Cancer Res. 1995;55:1152–1159.
22 Wolf DA, Wang S, Panzica MA, Bassily NH, Thompson NL. Expression of a highly conserved oncofetal gene, TA1/E16, in human colon carcinoma and other primary cancers: homology to Schistosoma mansoni amino acid permease and Caenorhabditis elegans gene products. Cancer Res. 1996;56:5012–5022.
23 Matsuo H, Tsukada S, Nakata T, Chairoungdua A, Kim DK, Cha SH, et al. Expression of a system L neutral amino acid transporter at the blood-brain barrier. Neuroreport. 2000;11: 3507–3511.
24 Duelli R, Enerson BE, Gerhart DZ, Drewes LR. Expression of large amino acid transporter LAT1 in rat brain endothelium. J Cereb Blood Flow Metab. 2000;20:1557–1562.
25 Killian DM, Chikhale PJ. Predominant functional activity of the large, neutral amino acid transporter (LAT1) isoform at the cerebrovasculature. Neurosci Lett. 2001;306:1–4.
26 Ritchie JW, Taylor PM. Role of the System L permease LAT1 in amino acid and iodothyronine transport in placenta. Biochem J. 2001;356:719–725.
27 Pineda M, Fernandez E, Torrents D, Estevez R, Lopez C, Camps M, et al. Identification of a membrane protein, LAT-2, that Co-expresses with 4F2 heavy chain, an L-type amino acid transport activity with broad specificity for small and large zwitterionic amino acids. J Biol Chem. 1999;274:19738–19744.
28 Rossier G, Meier C, Bauch C, Summa V, Sordat B, Verrey F, et al. LAT2, a new basolateral 4F2hc/CD98-associated amino acid transporter of kidney and intestine. J Biol Chem. 1999; 274:34948–34954.
29 Hoshoyamada M, Obinata M, Suzuki M, Endou H. Cisplatin-induced toxicity in immortalized renal cell lines established from transgenic mice harboring temperature sensitive SV40 large T-antigen gene. Arch Toxicol. 1996;70:284–292.
30 Takeda M, Tojo A, Sekine T, Hosoyamada M, Kanai Y, Endou H. Role of organic anion transporter 1 (OAT1) in cephaloridine (CER)-induced nephrotoxicity. Kidney Int. 1999;56:2128–2136.
31 Utsunomiya-Tate N, Endou H, Kanai Y. Tissue specific variants of glutamate transporter GLT-1. FEBS Lett. 1997;416:312–316.
32 Sadahiro S, Suzuki T, Tokunaga N, Yurimoto S, Yasuda S, Tajima T, et al. Detection of tumor cells in the portal and peripheral blood of patients with colorectal carcinoma using competitive reverse transcriptase-polymerase chain reaction. Cancer. 2001;92:1251–1258.
33 Snider JV, Wechser MA, Lossos IS. Human disease characterization: real-time quantitative PCR analysis of gene expression. Drug Discov Today. 2001;6:1062–1067.
34 Mizoguchi K, Cha SH, Chairoungdua A, Kim DK, Shigeta Y, Matsuo H, et al. Human cystinuria-related transporter: localization and functional characterization. Kidney Int. 2001;59:1821–1833.
35 Apiwattanakul N, Sekine T, Chairoungdua A, Kanai Y, Nakajima N, Sophasan S, et al. Transport properties of nonsteroidal anti-inflammatory drugs by organic anion transporter 1 expressed in Xenopus laevis oocytes. Mol Pharmacol. 1999;55:847–854.
36 Kim DK, Kanai Y, Choi HW, Tangtrongsup S, Chairoungdua A, Babu E, et al. Characterization of the system L amino acid

transporter in T24 human bladder carcinoma cells. Biochim Biophys Acta. 2002;1565:112–121.

37 Mastroberardino L, Spindler B, Pfeiffer R, Skelly PJ, Loffing J, Shoemaker CB, et al. Amino-acid transport by heterodimers of 4F2hc/CD98 and members of a permease family. Nature. 1998; 395:288–291.

38 Uchino H, Kanai Y, Kim DK, Wempe MF, Chairoungdua A, Morimoto E, et al. Transport of amino acid-related compounds mediated by L-type amino acid transporter 1 (LAT1): Insights into the mechanisms of substrate recognition. Mol Pharmacol. 2002;61:729–737.

39 Kim DK, Kanai Y, Chairoungdua A, Matsuo H, Cha SH, Endou H. Expression cloning of a Na^+-independent aromatic amino acid transporter with structural similarity to H^+/monocarboxylate transporters. J Biol Chem. 2001;276:17221–17228.

40 Prasad PD, Leibach FH, Mahesh VB, Ganapathy V. Relationship between thyroid hormone transport and neutral amino acid transport in JAR human choriocarcinoma cells. Endocrinology. 1994;134:574–581.

41 Vistica DT. Cytotoxicity as an indicator for transport mechanism: evidence that murine bone marrow progenitor cells lack a high-affinity leucine carrier that transports melphalan in murine L1210 leukemia cells. Blood. 1980;56: 427–429.

42 Ritchie JW, Peter GJ, Shi YB, Taylor PM. Thyroid hormone transport by 4F2hc-IU12 heterodimers expressed in *Xenopus* oocytes. J Endocrinol. 1999;163:R5–R9.

43 Kaira K, Oriuchi N, Imai H, Shimizu K, Yanagitani N, Sunaga N, et al. Prognostic significance of L-type amino acid transporter 1 expression in resectable stage I-III nonsmall cell lung cancer. Br J Cancer. 2008;98:742–748.

44 Nawashiro H, Otani N, Shinomiya N, Fukui S, Ooigawa H, Shima K, et al. L-type amino acid transporter 1 as a potential molecular target in human astrocytic tumors. Int J Cancer. 2006;119:484–492.

45 Usui T, Nagumo Y, Watanabe A, Kubota T, Komatsu K, Kobayashi J, et al. Brasilicardin A, a natural immunosuppressant, targets amino Acid transport system L. Chem Biol. 2006;13:1153–1160.

46 Kaira K, Oriuchi N, Otani Y, Shimizu K, Tanaka S, Imai H, et al. Fluorine-18-alpha-methyltyrosine positron emission tomography for diagnosis and staging of lung cancer: a clinicopathologic study. Clin Cancer Res. 2007;13:6369–6378.